www.ThePharmaJournal.com

The Pharma Innovation

ISSN (E): 2277-7695
ISSN (P): 2349-8242
NAAS Rating: 5.23
TPI 2023; SP-12(7): 2650-2655

www.thepharmajournal.com
Received: 01-04-2023
Accepted: 07-05-2023

Sidhartha Sekhar Swain
Division of Agricultural Engineering, ICAR-Indian Agricultural Research Institute, New Delhi, India

Tapan Kumar Khura
Division of Agricultural Engineering, ICAR-Indian Agricultural Research Institute, New Delhi, India

Pramod Kumar Sahoo
Division of Agricultural Engineering, ICAR-Indian Agricultural Research Institute, New Delhi, India

Hari Lal kushwaha
Division of Agricultural Engineering, ICAR-Indian Agricultural Research Institute, New Delhi, India

Roaf Ahmad Parray
Division of Agricultural Engineering, ICAR-Indian Agricultural Research Institute, New Delhi, India

Pankaj Malkani
Krishi Vigyan Kendra, Narkatiaganj, West Champaran (Dr RPCAU, PUSA, Samastipur, Bihar, India

Satish Devram Lande
Division of Agricultural Engineering, ICAR- Indian Agricultural Research Institute, New Delhi, India

Corresponding Author:
Sidhartha Sekhar Swain
Division of Agricultural Engineering, ICAR- Indian Agricultural Research Institute, New Delhi, India

Determination of physical and engineering properties of urea super granules (USG) for design of USG applicator

Sidhartha Sekhar Swain, Tapan Kumar Khura, Pramod Kumar Sahoo, Hari Lal Kushwaha, Roaf Ahmad Parray, Pankaj Malkani and Satish Devram Lande

Abstract
The efficacy of fertilizer deep placement in enhancing fertilizer utilization efficiency in wetland rice cultivation is well-established. However, challenges related to the properties of fertilizer granules have led to inconsistent results when using machines designed for their placement. Consequently, a recent Study aimed to determine the relevant physical and engineering properties of USG to aid in the design of a mechanical applicator. Various properties including size, shape, USG weight, bulk density, angle of repose, and coefficient of friction were assessed in a laboratory setting. Length, breadth, thickness, roundness, sphericity, weight and angle of repose on a mild steel surface of the USGs were found to be 18.37 ± 0.19 mm, 14.67 ± 0.27 mm, 7.1 ± 0.12 mm, 0.78 ± 0.03, 0.89 ± 0.02, 1.63 ± 0.47 and 32.65 ± 0.24 degrees respectively. The size and shape of the metering cup were established based on the maximum dimensions of the USGs. The design specifications for the metering cup, including cup number and cup size, were selected based on the dimensions of the USG and were determined to be 4 and 20.20 mm, respectively. Three different 3D printed metering device was used for performance evaluation based on cell fill, broken USG percent, missing index and multiple index. Result showed the optimum metering was obtained from the cup size of 20.20 mm.

Keywords: size, shape, USG weight, bulk density, angle of repose, coefficient of friction, cell fill, broken USG percent, missing index, multiple index

Introduction
Agriculture is the backbone of all societies across the globe. By 2050, the world population is projected to reach a peak of 9.7 billion and global agricultural production may need to expand by 60 to 110 percent to fulfil rising demand and ensuring food security (FAO 2009; Ray *et al* 2013) [9, 15]. Rice (*Oryza sativa* L.) is one of the most significant crops in the world and the main staple meal in Asia. It contributes 35–60% of the dietary calories consumed by more than 3 billion people worldwide (Fageria, 2003) [4]. To meet the food demands of a growing global population, it is predicted that by the year 2025, it will be necessary to produce roughly 60 percent more rice than is currently produced (Fageria, 2007; Normile, 2008) [5, 13]. In India, rice is one of the most important cereal crops and feeds more than 60 percent population. In India, 46.38 million hectares of land are used to grow rice, with a total annual production of 130.29 million tonnes in the year 2021-22 (Agricultural Statistics at a glance- 2022).
Under irrigated and advantageous rain-fed conditions, fertiliser, in particular nitrogen fertiliser, is the primary driving force to create significant rice yields. Urea in paddy cultivation is applied in 3 phases such that 50% prior to transplanting 25% during panicle initiation and rest 25% during flowering (S. Kumar & Shivay, 2009; Singh & Shivay, 2003) [12, 18]. Urea applied in form of prilled urea is often distributed in paddy fields. These methods are ineffective because plants only utilise roughly a third of the nitrogen fertiliser. The remaining amount is either immobilised in the soil or lost through runoff, leaching, and gaseous losses (D. Kumar *et al*., 2010) [11]. Nowadays, a slow release of urea by the deep placement of urea super granule (USG) is used as an effective N management strategy. According to Jaiswal & Singh, 2014 [9], deep placement of USG in India's irrigated rice successfully elevated N utilisation efficiency by 31.7% when compared to conventional applied urea.

Granule placement for USGs can be done manually or mechanically using applicators. When developing a USG metering device for an applicator, the physical and engineering characteristics of USGs are crucial. Length, width, thickness, geometric mean diameter (GMD), angle of repose, and coefficient of static friction are examples of physical qualities (Savant & Stangel, 1998) [17]. For the purpose of determining the design characteristics of an applicator, friction, bulk density, and true density were measured. The maximum length and thickness of USGs would have an impact on the depth and diameter of the metering cup (Savant & Stangel, 1990) [16]. The Singulation of USG in the hopper is influenced by both roundness and sphericity. Deflection angle and the flow parameters of the USGs in the hopper are influenced by the coefficient of static friction.

The physical and engineering characteristics of USG, which are crucial for constructing an appropriate applicator, are only vaguely known. These parameters, including size, shape, weight, bulk density, true density, angle of repose, and coefficient of static friction for USG, are the focus of this work. The design settings for the mechanical applicator were suggested based on the knowledge of these characteristics of USG.

Materials and Methods

USGs were supplied by m/s distinct horizon pvt ltd. Prilled urea was compressed to make USG. It is made up of sizable, distinct urea particles that are 46% nitrogen. In the laboratory of the Division of Agricultural Engineering, IARI, New Delhi, studies were conducted to measure the physical and engineering characteristics of USG. From the bulk of each sample, 20 USGs were chosen at random for each property measurement, and the mean value was calculated. Using a digital vernier calliper with a least count of 0.01mm, length, breadth, and thickness were measured (Fig 1). The roundness and sphericity of the USGs served to convey its shape.

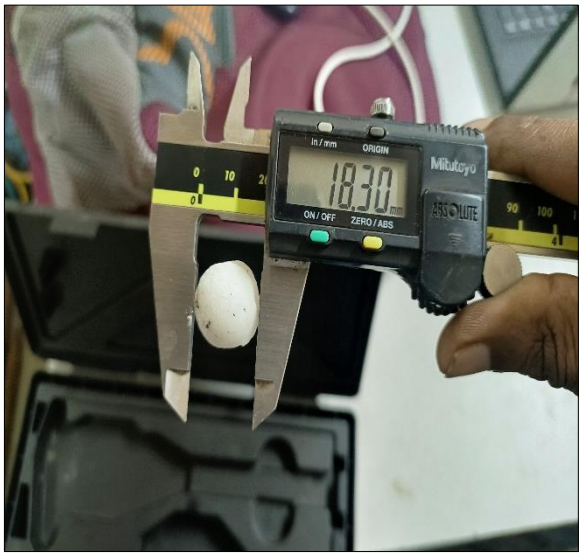

Fig 1: Measurement of dimensions of USG

Roundness was calculated by calculating the projected area and area of smallest circumscribing circle using equation 1 (Wadell, 1935) [19].

$$Rp = \frac{Ap}{Ac} \times 100 \quad (1)$$

Where,
Rp = Roundness, %
Ap = projected area, mm^2
Ac = area of smallest circumscribing circle, mm^2
Sphericity is calculated by the formula given in equation 2 (Wadell, 1935) [19].

$$\text{Sp} = Sp = \sqrt[3]{\frac{a \times b \times c}{a}} \quad (2)$$

Where,
Sp. = Sphericity
A = Longest intercept, mm
b = Longest intercept normal to a, mm,
c = Longest intercept normal to a and b, mm

USG bulk density was calculated using a measuring cylinder with a known volume. USGs were placed inside the measuring cylinder and volume was recorded (Fig 2). Upon emptying, weight of materials was measured and volume was calculated by using the formula given in equation 3. The identical process was carried out 30 times, and the mean value was calculated.

$$\text{BD} = \frac{W}{V} \quad (3)$$

Where,
BD = bulk density
W = weight of USG in measuring cylinder
V= volume acquired in cylinder by USG

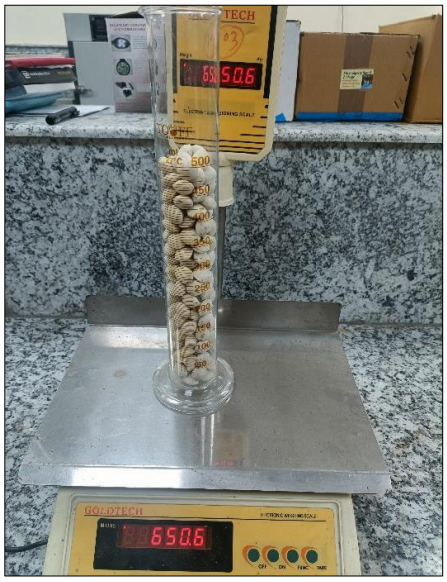

Fig 2: Measurement of bulk density

The tool, which was used to measure angle of repose, was a stand-mounted funnel with a movable neck aperture. Above the movable throat of the funnel was set a circular plate with four cantering arms. The funnel was stuffed full of USG by maintaining the throat close. To allow unrestricted flow of USGs over and around the plate fixed in the funnel, the throat was completely opened. A heap-cone of USGs eventually developed on the floor (Fig 3). Cone height and base diameter were measured. The identical technique was carried out 30 times, and the mean value was calculated by using the formula given in equation (4)

$$\Theta = \tan^{-1}\frac{2h}{d} \quad (4)$$

Where,
Θ = angle of repose (degree)
h = height of cone (cm)
d = diameter of base (cm)

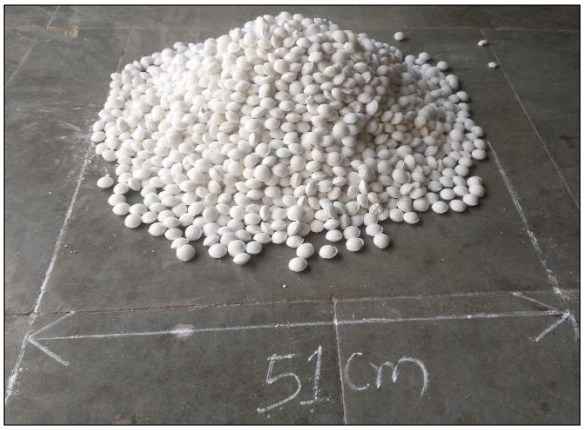

Fig 3: Heap of USG for coefficient of repose calculation

Using the inclined plane approach, the coefficient of static friction for USG on mild steel surface was determined. The surface where the material was maintained was horizontal, and the slope was gradually increased. The anticipated slide angle was noted. Tangent of angle was used to express the coefficient of static friction.
Hexane displacement method was used to determine the actual density of USGs. For the sample of 30 USGs, the volume and real density were assessed. Each USG weight was noted. The sample was submerged in a hexane-filled container. Fig 4 shows the volume of a single USG as well as the displacement volume of hexane for each. The weight to volume ratio of the sample was used to calculate true density. A total of 30 samples were observed, and the mean was used to determine the density of a single USG. The identical steps were performed for several treatments.

Fig 4: Hexane displacement method for calculation of true density

Design of metering device
The core of the applicator is the metering unit, which uniformly distributes USGs at a set rate with minimal damage and also regulates spacing between consecutive drops. To achieve positive metering, mechanical USG metering devices in an applicator typically feature cups on vertical rotors. The vertical rotor's circumference was surrounded by cups that were mounted as the vertical cup feed metering mechanism. A hopper containing USG was passed through by the vertical rotor with cup. USGs were taken out of the cups and dropped through two guides onto the top of the delivery funnel's inlet. To provide a consistent cup size for precise USG planting, the rotor and outer cups were 3D printed. The design of metering device involves determination of number of cells on the periphery of the rotor, shape and depth of the cups.
Let,
a = distance of coverage by a single USG, m
b = spacing between USGs, m

Number of USGs per $m^2 = \frac{1}{b \times a}$

Urea application rate in basal dose is 60 kg N ha^{-1}. As urea contains 46% N, the amount of Urea in basal application = 130 kg ha^{-1} = 0.013 kg m^{-2}
Drive to metering system was given through the electronic system which senses the drive from the transplanting shaft. One revolution of transplanting shaft transplants two seedlings. The layout of field has been presented in fig 5.

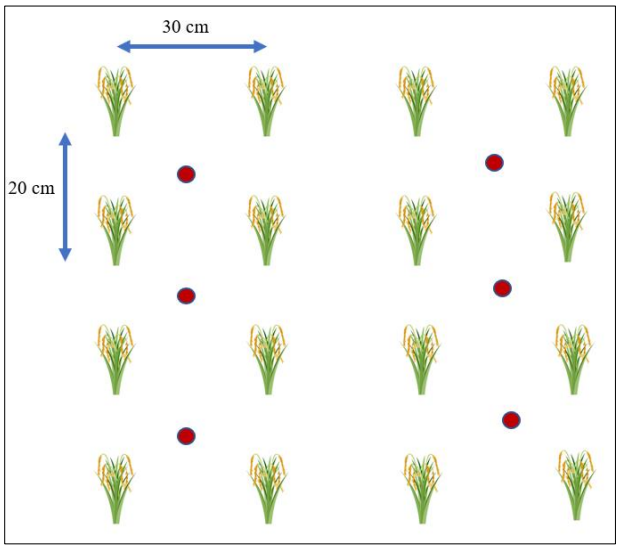

Fig 5: Layout of field application

The distance covered by one USG = (row to row distance + half the distance between row to row in the right side + half the distance between row to row in the left side) = 60 cm
Area covered by one transplanting = 0.12 m^2
Amount of urea applied = 13 × 0.12 = 1.56 g
Weight of one USG = 1.63 g
Number of USG applied for one transplanting = 1.56/1.63 ≈ 1
Metering roller was 3D printed with 4 cells on periphery and rotation was controlled by suitable electronic system. To find the ideal cup shape, three different sized cups were examined in a lab experiment for metering of USG. Shape and size of the cups were determined based on the physical properties of the USG.

Laboratory experiment
Parameters being measured in this study are cell fill, broken percentage, missing index, multiple index.
Determination of operating parameters

Width and depth of the cups are designed based on the physical properties of the USG. Size of the metering system should be 10% more than the size of the material to be metered (Guo *et al.*, 2021; Jinwu *et al.*, 2017) [7, 10]. Three metering roller was 3D printed with three different sizes. Mean largest length of USG is 18.37 mm. Three different rollers were fabricated with sizes as 90% of the largest length, equal to largest length and 10% higher than largest length. Table 1 represents research plan of laboratory testing

Table 1: research plan for laboratory study

S. No.	Parameters			
Independent parameters				
1	Cell size (mm)	16.53 mm (A)	18.37 mm (B)	20.20 mm (c)
Dependent parameters				
1	Cell fill			
2	Broken percent			
3	Missing percent			
4	Multiple percent			

Different sizes of Cell fill (Fc)

The cell fill of a metering device is defined as the total number of USGs delivered by the metering mechanism in a specific number of the metering system's revolutions divided by the total number of cells passed through the discharge point in equal no of revolutions. It is determined using Eq. (5) (Pareek *et al*. 2021b).

$$F_c = \frac{Ns \times 100}{Nc} \quad (5)$$

Where,

FC denotes the cell fill (%), Ns and Nc represent the total number of metered USGs and the total number of cells passing through the discharge point, respectively.

Broken percent (B_p)

During metering of USG, due to impact of metering mechanism on the material, breakage of material occurs. Broken percent was calculated by comparing the average weight of metered USG with the average weight of USG. Broken percent can be calculated by the formula given in Eq. (2)

$$B_p = \frac{m}{M} \times 100 \quad (2)$$

Where,

B_p denotes broken percent (%), m and M represent average weight of metered USG and average weight of USG respectively.

Missing index (I_{miss})

It is the percentage of USG spacing which are greater than 1.5 times the theoretical spacing. According to ISO 7256/1–1984(E) Standard missing index can be calculated by the following formula given in Eq. (3).

$$I_{miss} = \frac{L1}{N} \times 100 \quad (3)$$

Where,

I_{miss} denotes missing index, L_1 and N denote number of spacing greater than 1.5 times theoretical spacing and total number of observations respectively.

Multiple index (I_{mult})

It is the percentage of USG spacing which are lesser than or equal to 0.5 times the theoretical spacing. According to ISO 7256/1–1984(E) Standard multiple index can be calculated by the following formula given in Eq. (4).

$$I_{mult} = \frac{L2}{N} \times 100 \quad (4)$$

Where $I_{multiple}$ denotes multiple index, L_2 and N denote number of spacing lesser or equal to 0.5 times theoretical spacing and total number of observations respectively.

Results and Discussion

Physical and engineering properties

The size, shape, bulk density, seed weight, angle of repose and coefficient of static friction for USGs were measured and the average values were determined, as given in Table 2.

Table 2: Measured physical and engineering properties of USG

Parameters	Value
Length (mm)	18.37 ± 0.19
Breadth (mm)	14.67 ± 0.27
Thickness (mm)	7.1 ± 0.12
Sphericity	0.89 ± 0.02
Roundness	0.78 ± 0.03
Bulk density (g/cm3)	0.75 ± 0.01
True density(g/cm3)	1.26 ± 0.02
USG weight	1.63 ± 0.47
Angle of repose	32.65 ± 0.24

Effect of input parameters on dependent parameters

Effect of cell size on cell fill is presented in Fig 6. It was observed that with increase in cell size cell fill increases. It might be due to increase in cell size, more USGs were picked up resulting in increase in cell fill. It was also supported by (Hensh & Raheman, 2022) [8].

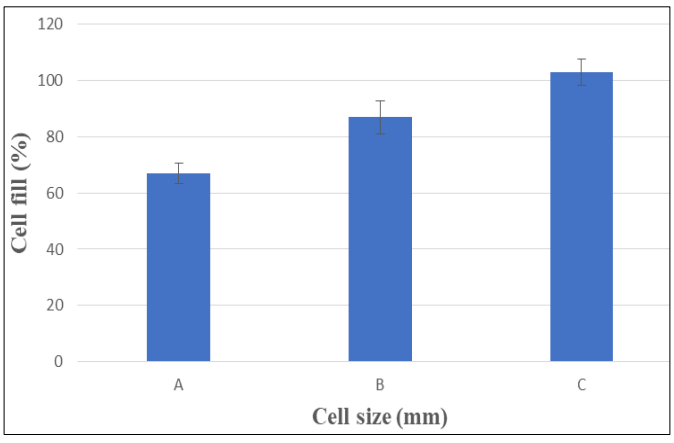

Fig 6: Effect of cell size on cell fill

Effect of cell size on broken percent has been presented in Fig 7. With increase in cell size, broken percent increased. It might be due to with increase in size metering came in contact with a greater number of USGs, which caused more broken percent.

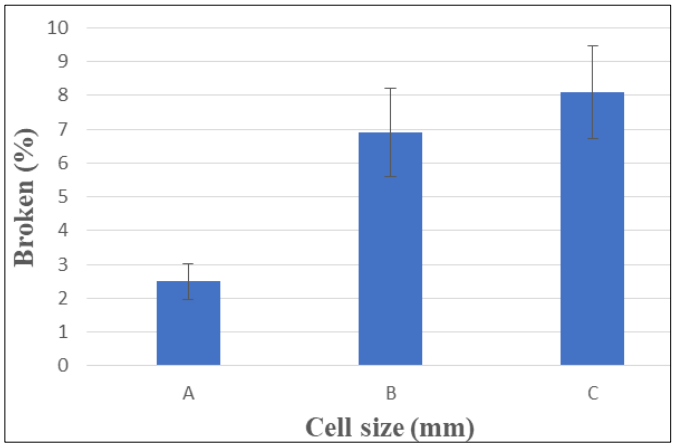

Fig 7: Effect of cell size on broken percent

Effect of cell size on missing percent of cell has been presented in Fig 8. As cell size decreased, miss index decreased. The probable cause might be with increase in cell size, probability of picking of USG is more which resulted in less missing index. It was also supported by the study conducted by (Bagherpour, 2019) [2].

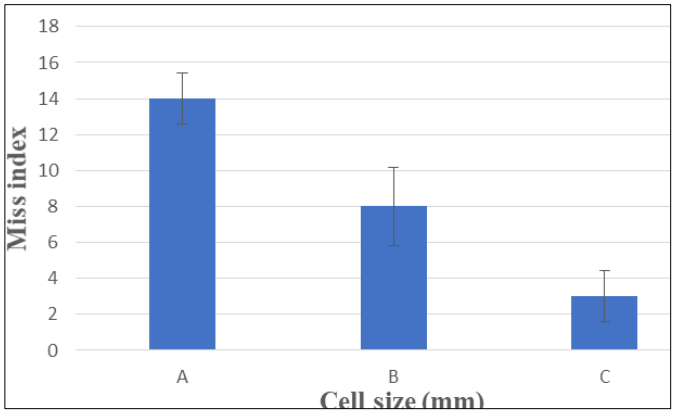

Fig 8: Effect of cell size on miss index

Effect of cell size on multiple index has been presented in Fig 9. It was observed that with increase in cell size, multiple index increased. The probable cause might be with increase in cell size, more number of USGs were picked by the cells resulting in more multiple index. Similar results also obtained by the study done by (Asl *et al*., 2019) [1].

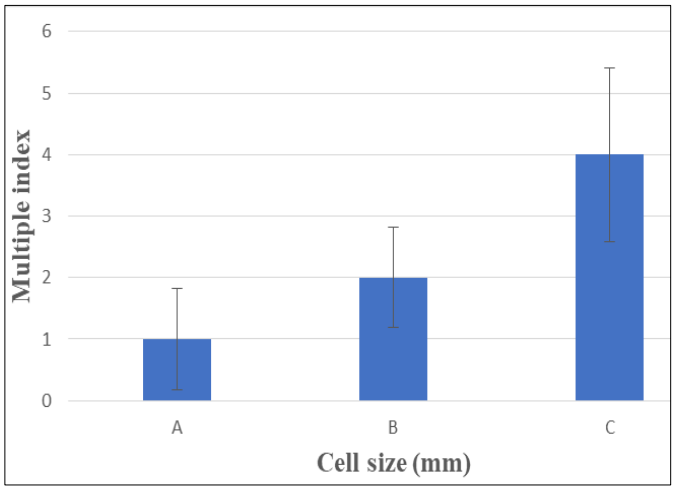

Fig 9: Effect of cell size on multiple index

Determination of optimum cell size

Table 3: Mean value of result obtained from the study has been presented

Size of cell	Cell fill	Broken percent	Missing index	Multiple index
A (16.53 mm)	67	2.5	14	1
B (18.37 mm)	87	6.9	8	2
C (20.20 mm)	103	8.1	3	4

Limiting value of performance evaluation was given by (Cay *et al*., 2018) [3] and presented in table 4.

Table 4: limiting values of performance criteria for precision metering

Missing index	Multiple index	Inference
< 0.7	< 0.7	Very good
≥ 0.7 to < 4.8	≥ 0.7 to < 4.8	Good
≥ 4.8 to < 7.7	≥ 4.8 to < 7.7	Moderate
> 7.7	> 7.7	Insufficient

By comparing values obtained in the study and values given by (Cay *et al*., 2018) [3], it was observed that c metering roller (20.20 mm size) performs satisfactorily and belong to good category.

Conclusion

In this study the physical and engineering properties of the USG were measured and metring roller for the efficient metering of USG was 3D printed. Different USG metering was evaluated based on the performance criteria of cell fill, broken percent, missing index and multiple index. Following conclusions were drawn from this study.

1. Mean value of length, breadth and thickness of the USGs were found to be 18.37 mm, 14.67 mm and 7.1 mm respectively.
2. Mean value of sphericity and roundness were found to be 0.89 and 0.78 respectively.
3. Mean value of unit weight, bulk density and true density were found to be 1.63 g, 0.75 g cm^{-3} cc and 1.26 g cm^{-3} respectively.
4. Angle of repose of USGs over 30 experiments was found to be 32.65°
5. Number of cells on the periphery of the metering roller was 4. With the optimum size of 20.20 mm.

This study will help the farmers, manufacturer and policy makers for efficient design of metering system.

Reference

1. Asl AR, Roudbari M, Esmailzadeh E. Fabrication and evaluation of vacuumed metering drum performance for row planting of soybean with grease belt. Agricultural Engineering International: CIGR Journal. 2019;21(4):96-106.
2. Bagherpour H. Modeling and evaluation of a vacuum-cylinder precision seeder for chickpea seeds, 2019, 21(4). http://www.cigrjournal.org
3. Cay A, Kocabiyik H, May S. Development of an electro-mechanic control system for seed-metering unit of single seed corn planters Part I: Design and laboratory simulation. Computers and Electronics in Agriculture. 2018;144:71-79. https://doi.org/https://doi.org/10.1016/j.compag.2017.11.

035.
4. Fageria NK. Plant tissue test for determination of optimum concentration and uptake of nitrogen at different growth stages in lowland rice. Communications in Soil Science and Plant Analysis. 2003;34(1-2):259-270.
5. Fageria NK. Yield physiology of rice. Journal of Plant Nutrition. 2007;30(6):843-879.
6. FAO U. Global agriculture towards 2050. FAO Rome; c2009.
7. Guo H, Cao Y, Song W, Zhang J, Wang C, Wang C, *et al*. Design and simulation of a garlic seed metering mechanism. Agriculture. 2021;11(12):1239.
8. Hensh S, Raheman H. Laboratory Evaluation of a Solenoid-Operated Hill Dropping Seed Metering Mechanism for Pre-germinated Paddy Seeds. Journal of Biosystems Engineering, 2022;47(1). https://doi.org/10.1007/s42853-021-00124-8
9. Jaiswal VP, Singh GR. Performance of urea super granule and priHed urea under different planting methods in irrigated rice (*Oryza sativa*); c2014.
10. Jinwu W, Han T, Jinfeng W, Xin L, Huinan H. Optimization design and experiment on ripple surface type pickup finger of precision maize seed metering device. International Journal of Agricultural and Biological Engineering. 2017;10(1):61-71.
11. Kumar D, Devakumar C, Kumar R, Das A, Panneerselvam P, Shivay YS. Effect of neem-oil coated prilled urea with varying thickness of neem-oil coating and nitrogen rates on productivity and nitrogen-use efficiency of lowland irrigated rice under Indo-Gangetic plains. Journal of Plant Nutrition. 2010;33(13):1939-1959. https://doi.org/10.1080/01904167.2010.512053
12. Kumar S, Shivay YS. Effect of eco-friendly modified urea materials and nitrogen levels on growth and productivity of Aromatic hybrid and an aromatic high yielding variety of rice. Ann. Agric. Res. New Series. 2009;30(1-2):4-8.
13. Normile D. Reinventing rice to feed the world. American Association for the Advancement of Science; c2008.
14. Outlook IE. AGE. IEA: Paris. France; c2019.
15. Ray DK, Mueller ND, West PC, Foley JA. Yield Trends Are Insufficient to Double Global Crop Production by 2050, 2013;8(6). https://doi.org/10.1371/journal.pone.0066428
16. Savan NK, Stangel PJ. Deep placement of urea super granules in transplanted rice: Principles and practices. Fertilizer Research. 1990;25(1):1-83. https://doi.org/10.1007/BF01063765
17. Savant NK, Stangel PJ. Urea briquettes containing diammonium phosphate: A potential new NP fertilizer for transplanted rice. Nutrient Cycling in Agro ecosystems. 1998;51(2):85-94. https://doi.org/10.1023/A:1009721419639
18. Singh S, Shivay YS. Coating of prilled urea with ecofriendly neem (*Azadirachta indica* A. Juss.) formulations for efficient nitrogen use in hybrid rice. Acta Agronomica Hungaric. 2003;51(1):53-59. https://doi.org/10.1556/AAgr.51.2003.1.7
19. Wadell H. Volume, shape, and roundness of quartz particles. The Journal of Geology. 1935;43(3):250-280.